Research Article

Unraveling the Role of H₂ and NH₃ in the Amination of Isohexides over a Ru/C Catalyst

Hang Hu,[⊥] Muhammad Akif Ramzan,[⊥] Raphael Wischert,* François Jerôme, Carine Michel,*
Karine de Oliveira Vigier,* and Marc Pera-Titus*

Read Online

ACCESS | Metrics & More | Article Recommendations | Supporting Information

ABSTRACT: The direct amination of biomass-derived isohexides with NH₃ over a Ru/C catalyst was systematically investigated to understand the role of H₂ and NH₃ in the production of isohexide diamines vs aminoalcohols, i.e., the transformation of one or both OH-groups in isohexides into NH₂ groups. Only aminoalcohols with an *exo*-OH group were generated starting from isosorbide, which contains both an *exo*-OH and an *endo*-OH group, while a moderate yield of diamines was obtained from isomannide with two *endo*-OH groups due to the higher reactivity of the latter. The main byproducts were identified, including a variety of N- and O-containing cyclic compounds, such as 2,5-dimethylpyrrolidine, that arise from a decomposition path driven by hydrolysis/hydro-deoxygenation of a tricyclic amine intermediate. By combining

density functional theory calculations with microkinetics, NH₃ was found to adsorb strongly on the catalyst surface and generate adsorbed NH₂ and NH species with variable coverage depending on the temperature and the nominal H₂/NH₃ ratio. Isomerization of isohexides was greatly suppressed by adsorbed NH₃. Meanwhile, adsorbed NH₃ discouraged the formation of byproducts driven by competing side reactions promoted by H₂. The H₂/NH₃ ratio, which conditions the distribution of NH₂ and NH species on the Ru surface, influences drastically the catalytic performance.

KEYWORDS: isohexides, amination, hydrogen, ammonia, ruthenium, catalytic mechanism
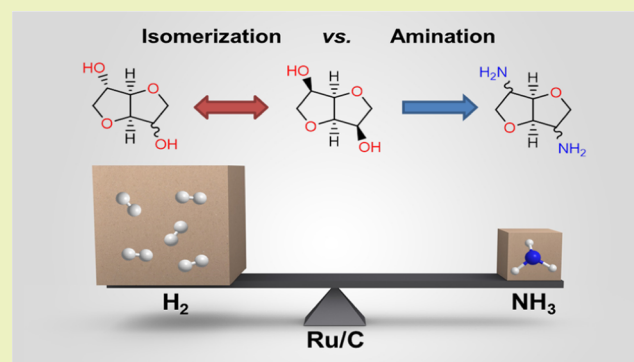
INTRODUCTION

Amines are essential building blocks in the chemical industry that are used as intermediates for the synthesis of polymers, surfactants, dyes, pharmaceuticals, and agrochemicals.[1,2] Traditionally, aromatic and aliphatic amines are industrially manufactured using synthetic routes encompassing petrochemical precursors.[3] However, the synthesis of value-added N-compounds from biomass has grown considerably, and more sustainable routes for transforming biobased platform molecules into useful amines have been sought.[4−10]

Isosorbide (IS) along with its isomers isomannide (IM) and isoidide (II), collectively referred to as isohexides, constitute a group of biobased platform chemicals that have gained interest as potential replacements to fossil-fuel-based products.[5,11,12] Isosorbide is produced at an industrial scale from polysaccharides. In particular, IS and its diamine derivatives show great interest in manufacturing biobased polymers such as polyurethanes, polymethacrylates, and polyamides.[8,13−15] The three isohexides differ in the relative configuration of the two secondary OH groups: IS has OH groups in opposite (*endo-exo*) orientations relative to the ring skeleton, while IM (*endo–endo*) and II (*exo–exo*) have OH groups pointing in the same direction relative to the ring skeleton (Scheme 1A). Unlike

exo-OH groups, *endo*-OH groups are better positioned to engage in intramolecular hydrogen bonding with the oxygen atoms of the adjoining furan ring.[16−19] These structural differences lead to differences in the physicochemical properties and reactivity of isohexides.[19,20]
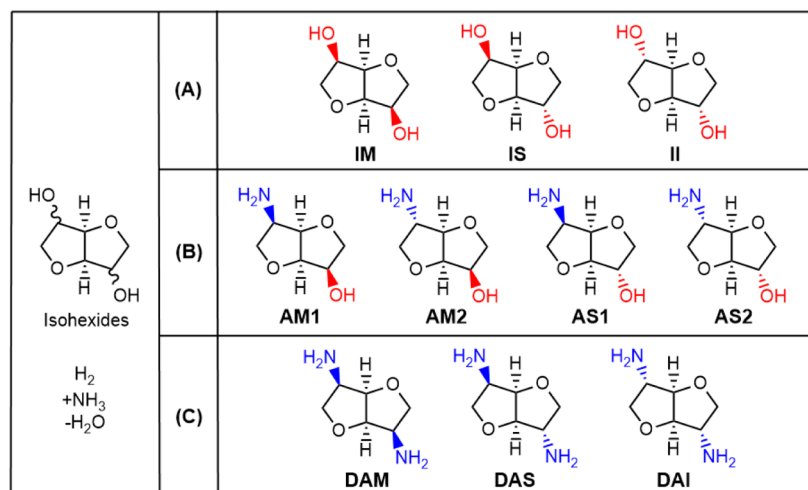
Diamines can be prepared from isohexides using poorly sustainable synthetic routes encompassing a large number of steps. The first studies reported the transformation of the OH groups of the isohexides into diamines with high yield and good stereocontrol by intermediate tosylation into good leaving groups. Montgomery, Bashford, and Wiggins prepared 2,5-ditosyl isosorbide and isomannide. Further treatment with NH₃ in methanol at 170 °C for 30 h resulted in isosorbide and isomannide diamines with 60 and 80% yields, respectively.[21,22] Cope and Shen developed an alternative route encompassing nucleophilic substitution of 2,5-ditosyl isosorbide with

Scheme 1. Products Obtained from the Direct Amination of Isohexides with NH$_3$ over Ru/C[a]

[a](A) isohexide isomers, (B) isohexide monoamines, and (C) isohexide diamines.

potassium phthalimide in DMF via an S$_N$2 mechanism, followed by deprotection with hydrazine hydrate.[19] This route is limited by the low overall yield (<4%) and the toxicity of hydrazine. Van Es and co-workers reported DMSO as a convenient solvent in the nucleophilic substitution step to avoid byproduct formation due to hydrolysis.[23] Besides, a mixture of HCl/glacial acetic acid was used instead of hydrazine, followed by treatment with basic ion exchange resin, leading to a 66% overall yield. Van Es and co-workers also reported benzylamine as an alternative to potassium phthalimide.[24] Further hydrogenolysis in ethanol of the as synthesized isohexide benzyldiamines over Pearlman's catalyst [Pd(OH)$_2$/C] resulted in isosorbide and isoidide diamines with 90% overall yield, together with an aziridine byproduct. Kuszmann and Medgyes reported the synthesis of isomannide diamines by IM conversion into bismesylates, followed by nucleophilic substitution with azide and hydrogenation.[25] Despite the high yield achieved (88%), this route is limited by the explosive behavior of azides, which discourages its application for large-scale diamine production.

As an alternative to the above routes, the synthesis of isohexide diamines by the direct amination of alcohols with NH$_3$ is an attractive option since the reaction proceeds in a single step and water is generated as the main byproduct. The direct amination of isohexides is regarded to proceed via a hydrogenation–rehydrogenation pathway (i.e., H$_2$-borrowing hydrogen).[26,27] This pathway, also at play in isohexide isomerization under H$_2$, encompasses alcohol dehydrogenation over a catalyst to generate a ketone intermediate that undergoes condensation with NH$_3$ to produce an imine. Subsequent hydrogenation of the imine with the stored H$_2$ affords the amine product. The direct amination of isosorbide IS with NH$_3$ to diamines was first described by Beller et al. using a Ru(CO)ClH(PPh$_3$)$_3$ complex combined with a Xantphos ligand.[4] The catalyst operated at 170 °C without exogenous H$_2$, providing a mixture of diamines with 96% yield at full IS conversion. However, the product distribution was not reported. Vogt et al. reported the direct amination of isomannide IM to isohexide diamines using Ru$_3$(CO)$_{12}$ and PNP pincer-type ligands with 96% yield.[28] The molar ratio between diamino isosorbide, isoidide, and isomannide after the reaction was 47:38:16, which is similar to the thermodynamic

ratio achieved between IS, II, and IM achieved after isomerization under H$_2$ (i.e., 39:55:6).[29,30] A similar catalytic system was patented in 2014 for the catalytic amination of isohexides in organic solvents and with different PNP pincer-type ligands.[31] This system produced a distribution of aminoalcohol and diamine products with a 60:40 molar ratio. Recently, Popowycz and co-workers described the amination of IS and IM with benzylamine using an Ir complex and diphenylphosphate, followed by hydrogenation.[32] In this route, only endo-OH groups were reactive, and benzyldiamine products could be accessed from IM with 59% yield.

The synthesis of amines from isohexides has also been attempted using heterogeneous catalysts. The efforts to date have concentrated on the amination of isohexides with NH$_3$ over Ru/C in water.[33,34] Unlike with ruthenium complexes, 4 aminoalcohols with different stereochemistry were obtained as main products (Scheme 1B), together with small amounts of diamines (Scheme 1C). The product distribution varied depending on the isohexide isomer. The amination of IS produced only aminoalcohols AS1 and AS2 with unreacted exo-OH and trace amounts of II, showing that endo-OH groups are reactive, while exo-OH groups are not. The conversion of IS increased with the H$_2$ pressure in the range of 0–10 bar, whereas it was unchanged at about 70% in the H$_2$ pressure range of 10–30 bar. In the case of IM, aminoalcohols AM1 and AM2 were obtained as the main products. Noticeably, the second endo-OH was barely aminated, with little formation of diamines (DAM, DAS, and DAI). Although the reaction did not require exogenous H$_2$, increasing the H$_2$ pressure above 10 bar led to higher conversion (increasing almost linearly with the H$_2$ pressure in the 10–40 bar range), but to the detriment of selectivity. A slight decline of the amine yield was observed, while a considerable amount of isomers, mainly II, were obtained due to competing reactions between isomerization and amination.

Herein, we present a combined experimental and computational study to rationalize the role of H$_2$ and NH$_3$ in the direct amination of isohexides over Ru/C. In particular, we investigated the influence of the isomerization reaction on the direct amination of IM and the nature of byproducts generated during amination.
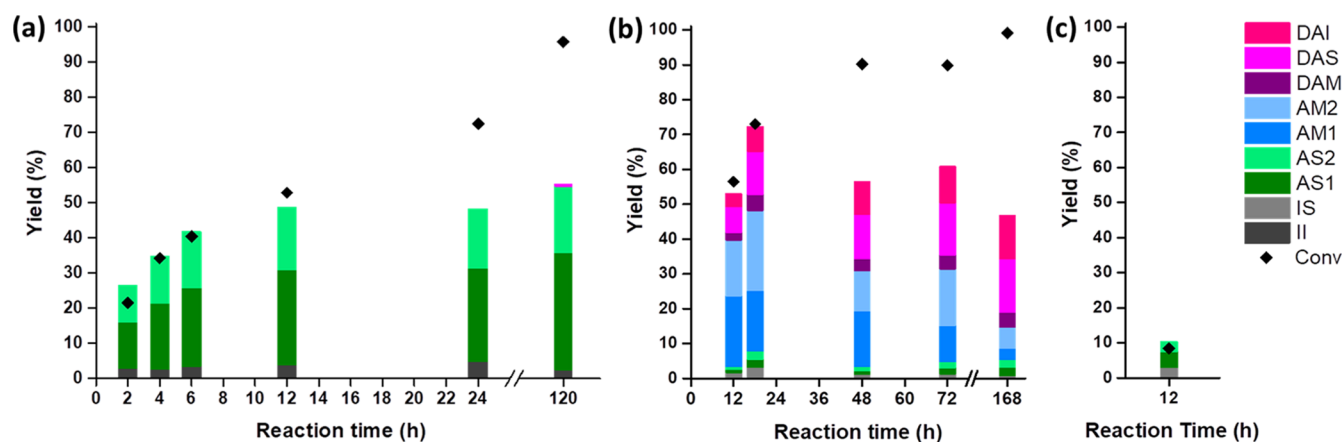
Figure 1. Kinetic profiles for the direct amination of (a) isosorbide IS, (b) isomannide IM, and (c) isoidide II, with NH_3. Reaction conditions: 1 g isohexide, 15 mL $NH_3 \cdot H_2O$ (25 wt %), pH = 13.5, 0.2 g Ru/C (5 wt %), 10 bar H_2, and 180 °C.
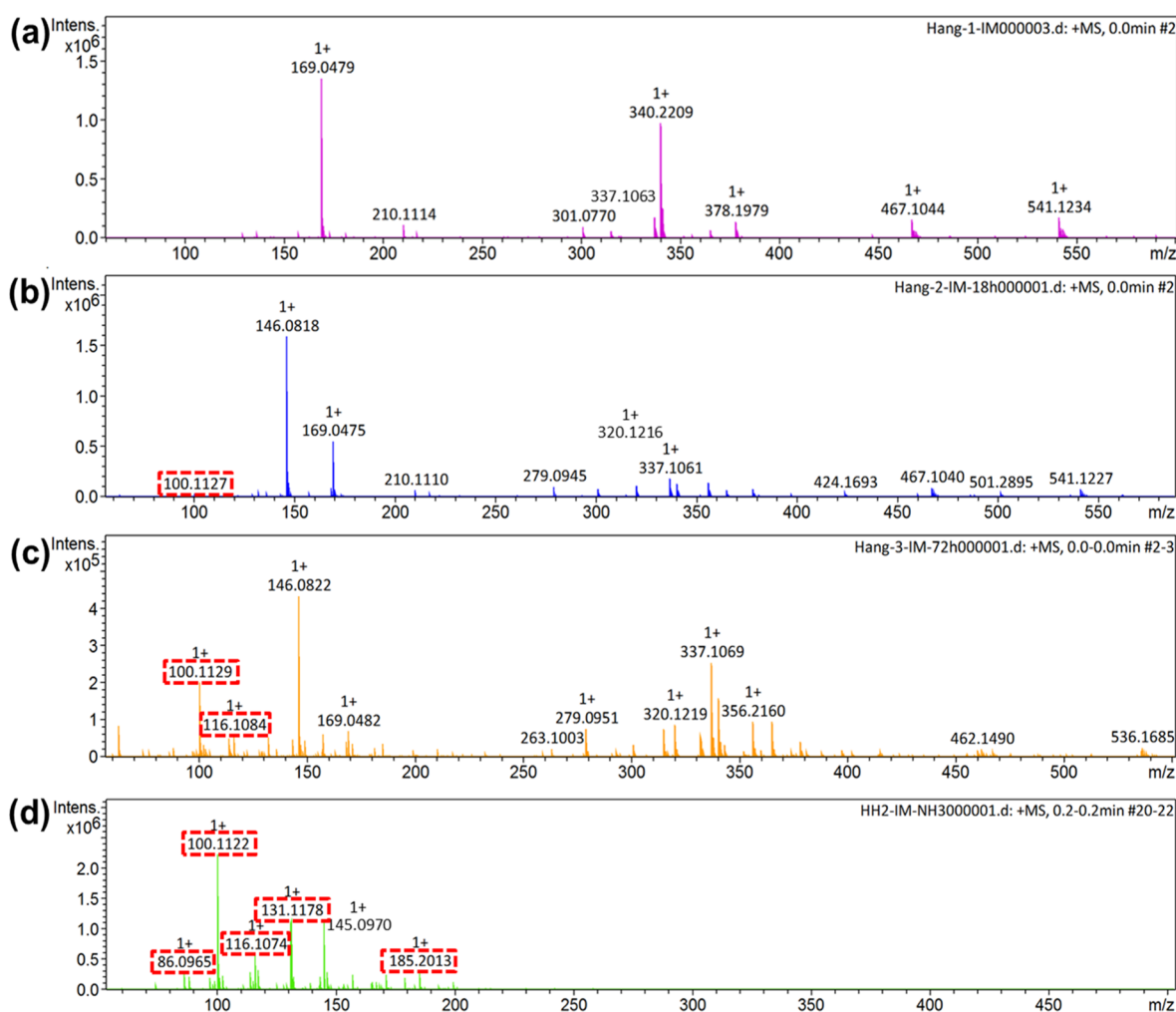
Figure 2. Mass spectra of (a) initial isomannide IM solution and reaction mixture obtained from the amination of IM after (b) 18, (c) 72, and (d) 168 h. Reaction conditions: 1 g IM, 15 mL $NH_3 \cdot H_2O$ (25 wt %), 0.2 g Ru/C (5 wt %), 10 bar H_2, and 180 °C. A higher concentration was used for the injected solution to obtain the mass spectrum (d) (0.5 mg/mL vs 0.1 mg/mL).

■ RESULTS AND DISCUSSION

Influence of the Substrate on the Catalytic Performance. First, we measured the kinetic profiles for the direct amination of IS, IM, and II with NH_3 at 180 °C (Figure 1). The product distribution varies depending on the starting isomer used. The amination of isosorbide IS only generates two aminoalcohols with *exo*-OH (i.e., AS1 with *endo*-NH_2 and AS2 with *exo*-NH_2) and very little II (Figure 1a). The complete absence of aminoalcohols with *endo*-OH (AM1 and AM2) clearly shows the low reactivity of the *exo*-OH groups, which is consistent with earlier observations by Pfützenreuter

Table 1. Possible Structures of C6−C4 Byproducts Detected during the Amination of IM, as Suggested by MS[a]

[a]The most likely structures are circled by a dashed orange line. Unsaturation degree $\Omega = (C \times 2 + 2 H + N)/2$.
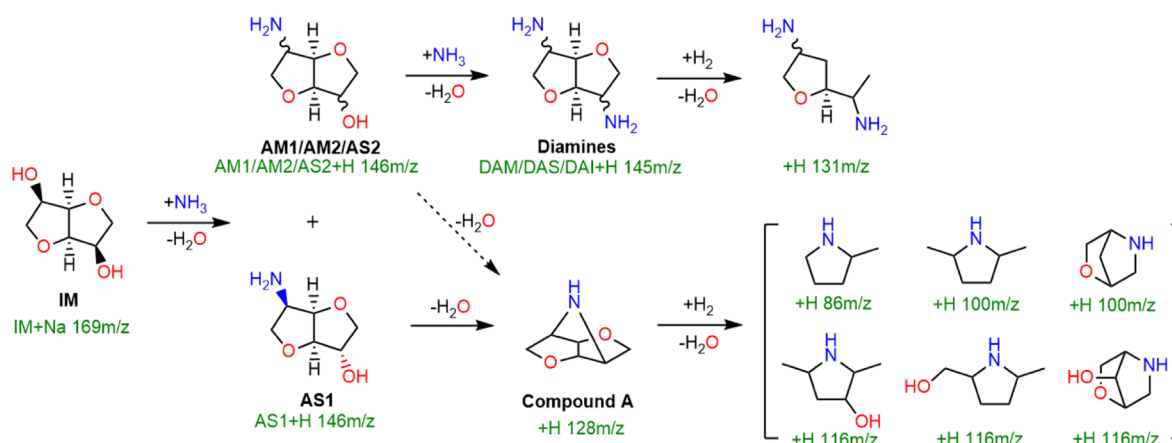

Figure 3. Proposed reaction routes for the formation of detected byproducts during the amination of IM.

and Rose.[33] The amination reaction is complete at *ca.* 50% conversion of IS, i.e., after 12 h. Extending the reaction time to 120 h promotes the conversion of IS to almost 100%. The combined yield of aminoalcohols (AS1 and AS2) keeps almost unchanged at 50% to the detriment of the formation of byproducts, and only a very small amount of diamines (0.7%) is formed.

Starting from isomannide IM, the main products obtained after 12 h are aminoalcohols with *endo*-OH (i.e., AM1 with *endo*-NH₂ and AM2 with *exo*-NH₂) and diamine products DAM, DAS, and DAI, with an overall yield of ~70% after 18 h at ~70% IM conversion (Figure 1b). By contrast with the absence of diamines when starting from isosorbide IS (Figure 1a), this confirms the higher reactivity of *endo*-OH vs *exo*-OH groups. While the IM conversion gradually increases to completion after 168 h, the total yield of amines decreases, suggesting that the aminoalcohols AM1 and AM2 are not stable for extended times under the reaction conditions. After 168 h, more than 50% of IM is converted to byproducts, which is very similar to what was observed for IS (see Figure 1a). However, the diamine-to-aminoalcohol ratio increases over time while keeping the total yield of diamines almost

unchanged, suggesting a slow conversion of the aminoalcohols to diamines over longer periods of time.

The above trends for IM and IS might be explained by the conversion of aminoalcohols and diamines into byproducts and/or by poisoning of Ru/C by excess NH₃, thus limiting the adsorption of H₂ and isohexides or favoring the degradation of isohexides. These hypotheses will be discussed in the forthcoming sections.

Finally, amination of isoidide II yields a very small amount of IS (3%) and aminoalcohols with *exo*-OH (AS1 and AS2, 7%) (Figure 1c), pointing out a first isomerization step of II to IS, followed by amination of the more reactive *endo*-OH groups of IS to yield said aminoalcohols. The amount of IS is surprisingly small since, in line of our previous study focusing on the isomerization of isohexides,[35] the isomerization equilibrium should be reached within 2 h at 160 °C, 10 bar H₂, again suggesting the inhibition of this reaction when NH₃ is present.

Analysis of the Byproducts Formed in the Amination of Isomannide. Since the mass loss in direct amination increases with the reaction time (Figure 1a,b), the amination of isomannide IM was stopped after 12, 72, and 168 h, and the reaction mixture was analyzed by MS to identify all possible

byproducts formed (Figure 2). The starting solution of IM shows IM + Na (m/z 169) and 2 IM + 2 Na + 2 H (m/z 340) peaks (Figure 2a). Other peaks (m/z 210, 279, 301, 329, 337, 356, 378, 467, and 541) are attributed to contamination derived from the MS instrument by comparison with blank tests (Figure S1). Aminoalcohol AS2 and diamine DAS solutions were also analyzed by MS, showing no fragment peaks (Figure S2). Aminoalcohols at m/z 146 (+H) and unreacted IM at m/z 169 (+Na) are visible in the reaction mixture after 12 h reaction (Figure 2b). The peak appearing at 145 (+H) m/z, which at first sight can be ascribed to a satellite of 146 m/z (+H), can be attributed to isohexide diamines. Besides contamination peaks, no product is detected above 200 m/z, indicating no condensation of any product, resulting in a good carbon balance. A higher aminoalcohol (146 m/z) to IM (169 m/z) ratio is observed after 72 h compared to 12 h (Figure 2c), which is consistent with a higher IM conversion. The peaks above 200 m/z are more visible according to the smaller intensity scale (10^5) used, but can still be attributed to contamination. Two obvious peaks at m/z 100 (+H) and 116 (+H) are observed in the reaction mixture, especially at longer reaction times, which can be attributed to byproducts (Figure 2b−d). After 168 h, isohexide diamines become the main products and are observed at m/z 145 (+H) (Figure 2d). Additional byproducts are visible at m/z 86 (+H), 131 (+H), and 185 (+H).

Table 1 lists the possible byproducts generated that are compatible with the MS spectra. All the compounds have at least one O- or N-containing heterocycle. To rationalize the formation of the most likely byproducts (highlighted with a dashed orange frame), plausible degradation routes from IM can be proposed (Figure 3). The byproduct with MW = 130 could be generated from hydrodeoxygenation of isohexide diamines since its peak at m/z 131 (+H) appears only after 168 h, while the conversion of IM already exceeds 90% after 48 h. We also identified 2,5-dimethylpyrrolidine, a bicyclic compound including a C5 N-heterocycle with MW = 99 and other byproducts with MW = 115 and MW = 85. All these byproducts could be formed from an intermediate tricyclic compound (i.e., 2,5-imino-1,4:3,6-dianhydro-2,5-dideoxy-D-mannitol, A, MW = 127), opening a path to degradation routes (and carbon loss) driven by ring opening, followed by hydrodeoxygenation, hydrogenolysis, and C−C cleavage.

The tricyclic compound A could be generated by internal nucleophilic substitution (S_N2) of AS1, exhibiting an *anti* configuration between the nucleophile (*endo*-NH$_2$) and the leaving group (*exo*-OH), with a Gibbs free energy of reaction $\Delta_r G = -10$ kJ mol^{-1} at 200 °C computed using the M06-2X functional. Water may facilitate proton shuttling from −NH$_2$ to −OH to yield compound A and H$_2$O. Another possibility is an internal substitution (S_N2) of DAS, with one *endo*-NH$_2$ and one *exo*-NH$_2$, to yield compound A and NH$_3$, but this reaction is predicted to be endergonic with $\Delta_r G = +3$ kJ mol^{-1} at 200 °C. Finally, compound A might also be obtained by internal nucleophilic substitution (S_N1) with an *endo*-OH or *endo*-NH$_2$ leaving group and still an *endo*-NH$_2$ as nucleophile in the AM1 aminoalcohol ($\Delta_r G = -13$ kJ mol^{-1}) and the DAM diamine ($\Delta_r G = -1$ kJ mol^{-1}). All in all, the most likely path based on the Gibbs free energy of the reaction appears to be the internal nucleophilic substitution in AS1 or AM1.

While we did not detect compound A, this compound has been reported by Bashford and Wiggins when reacting isoidide bistosylate with methanolic NH$_3$.[22] Compound A has also

been prepared by reacting isoidide bistosylate with benzylamine, followed by hydrogenolysis over a Pd(OH)$_2$ catalyst.[23] Overall, these studies suggest that compound A can be accessed in our reaction system either in the bulk alkaline solution or over the Ru/C catalyst at high IM conversion (>70%).

Role of NH$_3$ and H$_2$ in the Amination of Isomannide IM. *Effect of NH$_3$ and Aminoalcohols on the Amination of IM.* To assess the potential inhibition of aminoalcohols on the catalytic activity of Ru/C, the amination of isomannide IM was performed in the presence of aminoalcohol AS2 (with *exo*-NH$_2$) in the starting solution and in excess of NH$_3$ (Figure 4).
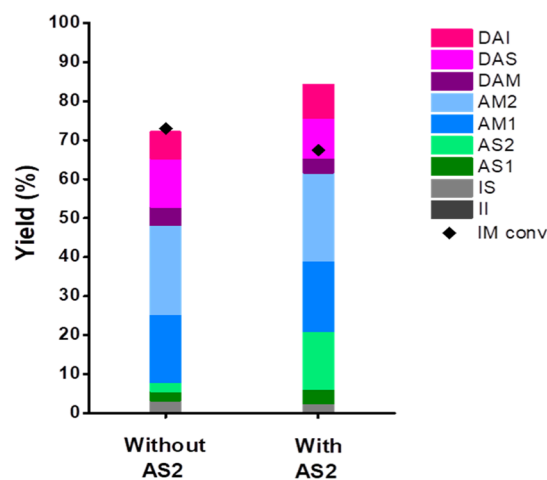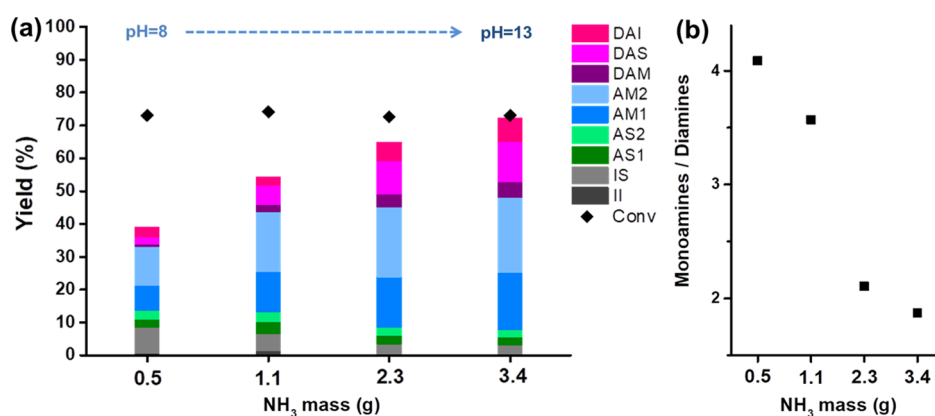

Figure 4. Conversion of isomannide IM and product distribution in the amination of IM without (left) and with (right) addition of 0.15 g AS2 (15 wt % to IM) to the starting solution. Reaction conditions: 1 g IM, 15 mL NH$_3$.H$_2$O (25 wt %), 0.2 g Ru/C (5 wt %), 10 bar H$_2$, 180 °C, and 18 h.

This aminoalcohol was chosen since it was found to be not reactive from the experiments using IS (Figure 1a). Only 15 wt % of AS2 based on IM (almost the same molar percentage) was added to the starting solution to prevent competitive adsorption with the substrate. Interestingly, AS2 did not react and did not exert any influence on the product distribution or IM conversion compared to the direct amination of pure IM. These results suggest that aminoalcohols do not inhibit the reaction.

To investigate the role of NH$_3$ on the catalytic activity and selectivity, the amination of IM was conducted at variable NH$_3$ loading in the reactor by diluting 25 wt % aqueous NH$_3$ with H$_2$O, while the H$_2$ pressure was kept unchanged at 10 bar (Figure 5). At about 70% conversion of IM, the total yield of amines increases with the NH$_3$ loading from 0.5 to 3.4 g, while the amount of isomerization products (IS and II) declines. In parallel, the aminoalcohols-to-diamines molar ratio decreases from 4.1 to 1.9. Interestingly, the more NH$_3$ is present, the higher the carbon balance, accompanied by an increase in the pH of the reaction mixture. These results underline the competitive role of hydrogenolysis/hydrodeoxygenation of IM over amination at lower NH$_3$ loadings, resulting in the formation of acid byproducts not detectable by MS (e.g., short-chain carboxylic acids) (Figure 3)[36] and promoting the isomerization of isohexides.[35]

Effect of H$_2$ Pressure on the Amination of Isomannide IM. The effect of H$_2$ pressure on the amination of isomannide IM

Figure 5. (a) Conversion of isomannide IM and product distribution, as a function of the amount of NH_3, in the direction of amination of IM. Reaction conditions: 1 g IM, 15 mL solvent, 15 to 2.2 mL $NH_3.H_2O$ (25 wt %), 0.2 g Ru/C (5 wt %), 10 bar H_2, 180 °C, and 18 h. (b) Molar ratio of aminoalcohols-to-diamine products as a function of the amount of NH_3.

was further investigated at constant NH_3 loading (3.4 g) (Figure 6). The IM conversion increases with the H_2 pressure
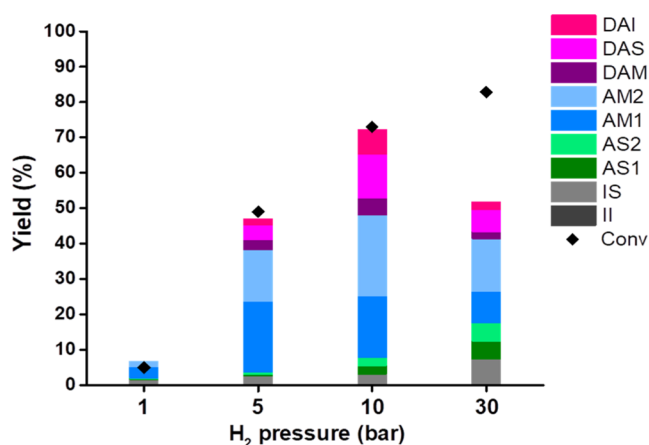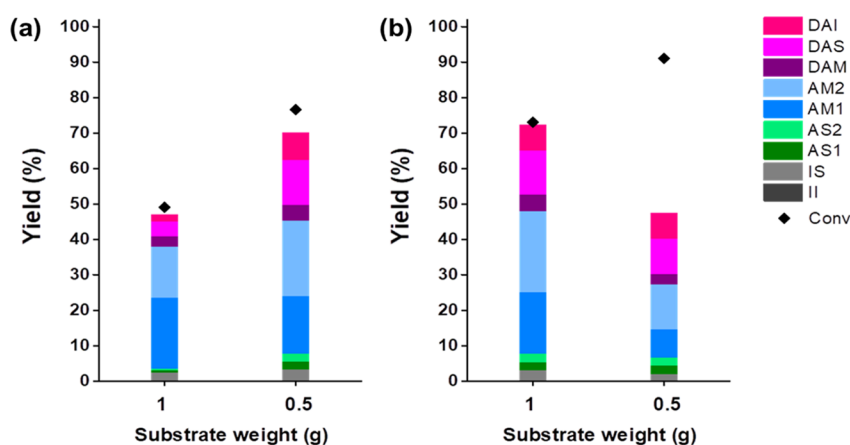

Figure 6. Conversion of isomannide IM and product distribution under different H_2 pressures. Reaction conditions: 1 g IM, 15 mL $NH_3.H_2O$ (25 wt %) (pH = 13), 0.2 g Ru/C (5 wt %), 180 °C, and 18 h.

from 1 to 30 bar, with a concomitant decrease of the diamine yield and carbon balance due to byproduct formation for a H_2

pressure higher than 10 bar. In parallel, IS is generated from the isomerization of IM, with a higher yield due to faster isomerization at higher H_2 pressures.[34] Subsequent amination of IS produces aminoalcohols AS1 and AS2. This observation is further confirmed by MS analysis of the reaction solution after amination of IM under 30 bar of H_2 (Figure S3). At this higher H_2 pressure, a new peak is observed at 132 m/z (+H), not listed in Table 1, which can be ascribed to ring-opening products of compound A, while another peak at m/z 100 is ascribed to a product originating from further hydrodeoxygenation. Additional byproducts originating from hydrodeoxygenation/hydrogenolysis at higher H_2 pressures are listed in the Supporting Information (Figure S4).

The effect of the H_2 pressure on the amination of IM was investigated at two different IM loadings (i.e., 0.5 and 1.0 g) while keeping the Ru/C loading constant at 0.2 g (Figure 7). Under 5 bar H_2 pressure, the IM conversion is 75% using 0.5 g of IM, whereas it decreases to 49% using 1.0 g of IM, while keeping in both cases a carbon balance higher than 90% (Figure 7a). The higher IM conversion in the former case can be attributed to a higher catalyst-to-substrate ratio. While under 10 bar H_2 pressure, the conversion is higher (90% for 0.5 g of IM and 70% for 1 g of IM), and the trend in the conversion is similar to that found for 5 bar H_2 pressure (compare Figure 7a,b). However, contrary to what was found

Figure 7. Conversion of isomannide IM and product distribution at 1 and 0.5 g IM under (a) 5 bar and (b) 10 bar H_2. Other reaction conditions: 15 mL $NH_3.H_2O$ (25 wt %) (pH = 12), 0.2 g Ru/C catalyst, 180 °C, and 18 h.

with 5 bar H_2 pressure, the total amine yield is much lower using 0.5 g of IM. An increase of the H_2 pressure from 5 to 10 bar enhances the rate of amination, resulting in an increase of the total yield of amines from 47% at 5 bar H_2 to 70% at 10 bar H_2. In contrast, using 0.5 g of IM, side reactions are strongly promoted by increasing the H_2 pressure from 5 to 10 bar. This results in a decline of the total yield of amines due to competitive hydrogenolysis/hydrodeoxygenation reactions of aminoalcohols or IM, leading to different byproducts (Figure 3).

Reactivity of Ketones. Finally, we studied the role of monoketones as intermediates during the amination of isomannide IM. The *endo*-OH monoketone was synthesized by oxidation of IM with 10 bar O_2 over Pt−Bi/C (see the Supporting Information for details), resulting also in the formation of the diketone. The IM/*endo*-OH ketone/diketone molar ratio of the resulting mixture was 26:48:10. This mixture was then subjected to reductive amination using aqueous NH_3 over Ru/C at 100 °C and 10 bar H_2 (Figure S5). Under such conditions, the reaction mixture is enriched with IM after 12 h, which can be attributed to the partial hydrogenation of the *endo*-OH group. Besides, two aminoalcohols with *endo*-OH (i.e., AM1 with *endo*-NH_2 and AM2 with *exo*-NH_2) are generated, as well as a few diamines.

We also investigated the product distribution in the reductive amination of the pure isohexide diketone over Ru/C. Despite full conversion of the diketone, neither isohexide monoketones nor amines are observed at 25 °C after 1 h or at 100 °C after 18 h. A dark brown-colored solution is obtained just by reacting the diketone with aqueous NH_3 over Ru/C and 10 bar H_2, suggesting fast imine formation, followed by polymerization.

The results above point out that the *endo*-OH monoketone is most likely an intermediate originating from IM dehydrogenation. However, the diketone is not expected to be generated on the catalyst surface during IM dehydrogenation and participate in the catalytic mechanism.

Competition of Amination and Isomerization of Isomannide over Ru/C. During the amination of isohexides, isomerization can also occur. In the absence of NH_3, the three isohexide isomers can interconvert over Ru/C under a pressure of H_2. In particular, we have recently shown that IS can isomerize, starting either from the *endo*-OH or *exo*-OH with a comparable energetic span.[35] In the absence of co-adsorbed H, chemisorbed monoketones are strongly bonded to the Ru surface because of the stabilizing interaction with the ether of the adjoining cycle. As a result, monoketones poison the Ru catalyst, with re-hydrogenation being the limiting process. In the presence of H_2, monoketones are less strongly adsorbed and are more easily re-hydrogenated, producing IS, IM, or II. The isomerization equilibrium is reached within 2 h at 160 °C, 10 bar H_2 (i.e., the II/IS/IM molar ratio of 61:35:4).

To rationalize the final distribution of products in the amination of isohexides, it is critical to understand the interplay between this reaction and the isomerization of isohexides, in the presence of both NH_3 and H_2. In this view, we first explored the evolution of IM over Ru/C at 200 °C in water solvent under 30 bar H_2 (Figure 8). In line with our previous study,[35] IM isomerizes into II and IS, reaching thermodynamic equilibrium after 2 h. Next, we reacted IM with a small amount of NH_3 (1 mL of 25 wt % $NH_3·H_2O$ instead of 15 mL in the previous experiments) in water (15 mL) at 200 °C under 30 bar H_2. Isomerization is suppressed
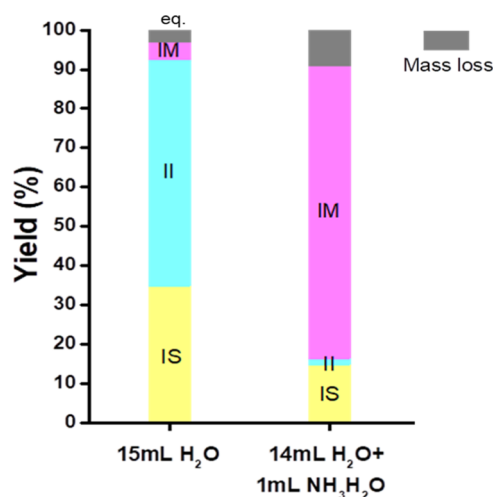

Figure 8. Product distribution and mass loss in the isomerization reaction of isomannide IM in the presence of NaOH (pH = 10) (left) and $NH_3·H_2O$ (25 wt %, 1 mL) (pH = 8) (right). Reaction conditions: 1 g IM, 15 mL solvent, 0.05 g Ru/C (5 wt %), 30 bar H_2, 200 °C, and 2 h.

and does not reach equilibrium. This observation is consistent with the low yield of isohexide isomers observed during amination in excess NH_3 and suggests strong inhibition of isomerization in the amination reaction.

We conducted two further catalytic tests on mixtures resulting from the amination reaction (Figure 9). In these tests, we kept the pH at basic conditions to discourage the side effects of the pH on the reactivity. We first carried out the amination of IM at 180 °C for 18 h (pH 13), and then, NH_3 was partially removed by bubbling N_2 for 6 h until the pH was 11. The resulting mixture was then reacted with 30 bar of H_2 (Step A, Figure 9a). The yield of isohexides and aminoalcohols remains almost unchanged, while the yield of diamines decreases slightly. NH_3 was further added to the reactor, and the amination reaction was resumed (Step B, Figure 9a), leading to a moderate increase of the yield of diamines. We conducted a second catalytic test at 180 °C for 18 h and then fully removed NH_3 under vacuum (pH 11) (Step A, Figure 9b). The yield of amines exhibits a remarkable decrease, especially in the case of diamines, reinforcing the idea that diamines are more vulnerable to H_2 than aminoalcohols over Ru/C. Besides, the ratio of AM2 (with one *exo*-NH_2) to AM1 (with one *endo*-NH_2) increases dramatically, either due to partial isomerization from AM1 to AM2 or due to a higher decomposition rate of AM1. The isomerization of IM is also inhibited in the presence of the amine products, as described above.

Understanding the Role of NH_3 and H_2 in IM Amination. To improve our understanding of the role of NH_3 and H_2 in isomannide IM amination over Ru/C, we performed density functional theory (DFT) calculations, complementing our previous studies focusing on the isomerization reaction.[35] Aminoalcohols are the main products of the amination reaction in the case of IS, with only traces of the desired diamines produced. Further reaction of the aminoalcohols to the desired diamine products is observed in the case of IM, but to a limited extent. Alcohol amination is a multistep process that starts with the OH scission activated by the Ru/C catalyst.[37] Considering the adsorption on Ru(0001) followed by the O−H scission (TS_{OH}), we compare IM with
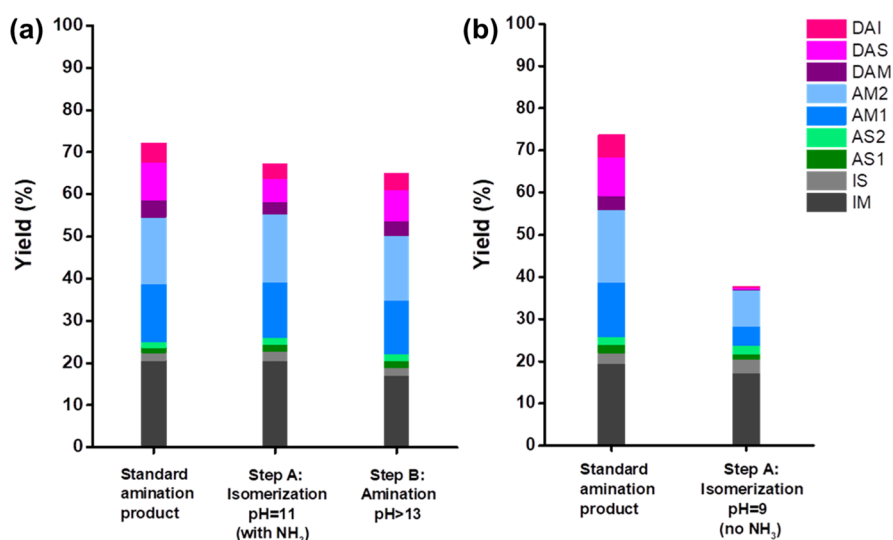
Figure 9. Product distribution in consecutive isomerization−amination tests. Step A reaction conditions: 15 mL mixture, 0.05 g Ru/C (5 wt %), 30 bar H_2, 200 °C, and 2 h. Step B reaction conditions: 15 mL mixture, 9 g NH_3, pH > 13, 0.2 g Ru/C (5 wt %), 10 bar H_2, 180 °C, and 18 h.
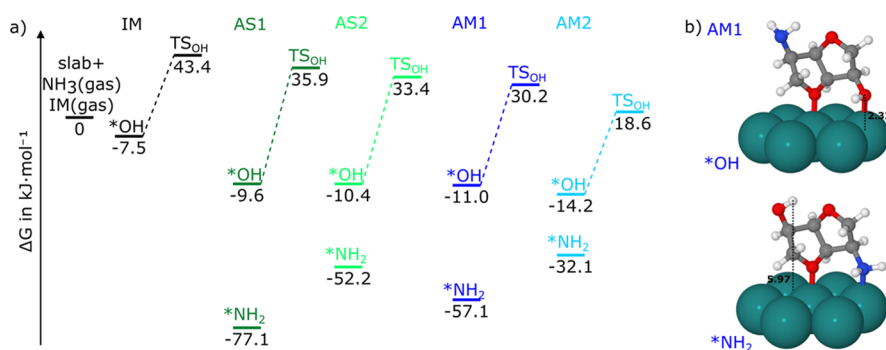

Figure 10. (a) Gibbs free energy profiles, including adsorption and O−H scission (TS_{OH}) of IM and the four aminoalcohol intermediates (AS1, AS2, AM1, and AM2) found in the amination reaction of isohexides. The entropic and enthalpic contributions were calculated at 200 °C and 1 atm using a harmonic ideal gas approximation. Reference energy is the pristine Ru(0001) slab, IM in the gas phase, and NH_3 in the gas phase. When considering the aminoalcohols, the water molecule generated by the amination of IM is set in the gas phase. (b) Optimized structures of AM1 on Ru(0001). N in blue, O in red, C in gray, H in white, and Ru in green. Only selected top-most atoms of the Ru slabs are shown. The distance between the H of the −OH and the average height of the topmost layer of Ru is indicated with a black dash and given in Å. *OH and *NH_2 stand for adsorption configuration through OH and NH_2 functional groups, respectively.

the four aminoalcohol intermediates (i.e., AS1, AS2, AM1, and AM2, see Scheme 1). The corresponding Gibbs free energy profiles are provided in Figure 10a. IM adsorbs weakly by building two Ru−O weak bonds with one O-ether and one hydroxyl group. The O−H breaks with an activation energy of 33 kJ mol^{-1}. Adsorption of aminoalcohols is clearly much more favorable via their NH_2 group (NH_2*) than via their OH group (OH*) by at least 25 kJ mol^{-1}, which means that the OH group points away from the catalyst surface in the most stable adsorption mode (>5 Å, see illustration for AM1 in Figure 10b). Starting from the OH* adsorption mode, the O−H scission barrier is comparable to that found for IM (around 30 kJ mol^{-1}). However, the overall barrier rises to at least 59 kJ mol^{-1} by including the adsorption equilibrium between the most stable adsorption mode (NH_2*) and the least stable but reactive adsorption mode (OH*). In other words, amino-alcohols are predicted to be less reactive than IM in agreement with our experimental findings (formation of aminoalcohol is comparatively easy, while further reaction to diamines is strongly inhibited), and this is mainly related to the over-stabilizing adsorption through the amino substituent (NH_2*)

compared to the reactive adsorption through the alcohol substituent (OH*).

According to our previous work on the isomerization of isohexides over Ru/C (i.e., without NH_3),[35] exogenous H_2 is necessary to promote the isomerization of the isohexides (IS/ II/IM). DFT calculations highlighted that isomerization is facilitated on a Ru(0001) surface covered by H compared to a pristine surface.[35] To elucidate the impact of NH_3 on the isomerization of isohexides, we investigated the fate of NH_3 on Ru(0001). Given the weak Gibbs free adsorption of IM (−8 kJ mol^{-1}) compared to that of NH_3 (−37 kJ mol^{-1}), the co-adsorption of IM was ruled out in our calculations. The corresponding reaction profile is shown in the Supporting Information (Figure S7). NH_3 adsorbs strongly on Ru(0001) and easily dissociates into NH_2, NH, and N (barrier < 110 kJ mol^{-1}). Noteworthy, recombination of N into N_2 is limited by a very high barrier (295 kJ mol^{-1}). These results are in agreement with previous work on the synthesis of NH_3 and its decomposition over Ru surfaces.[38,39] These aforementioned surface species could be responsible for surface poisoning, as confirmed by microkinetic modeling, where the steady state
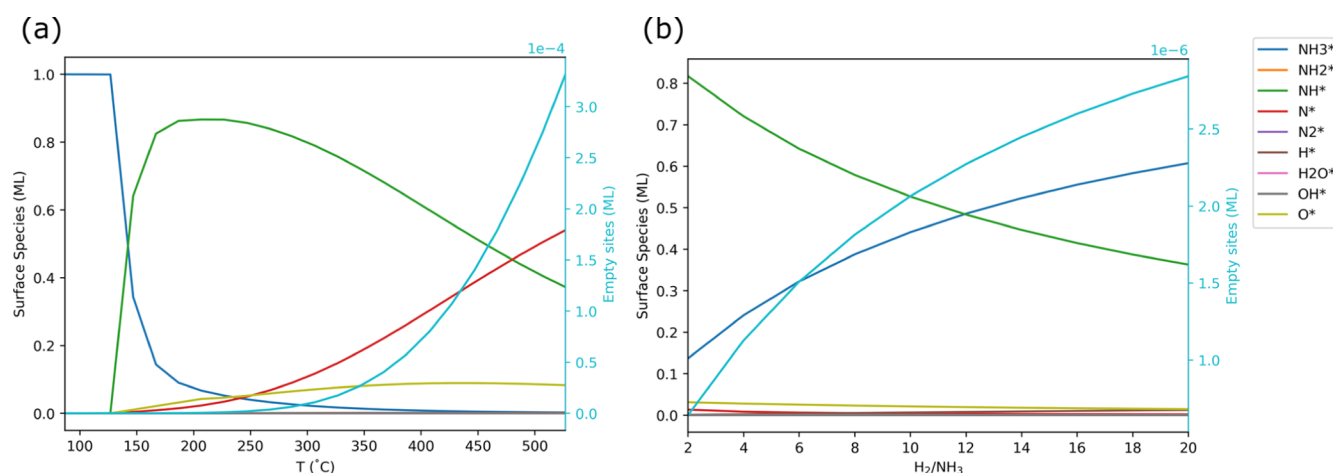
Figure 11. Predicted coverage obtained from microkinetics in combination with the energy barriers computed at the DFT level (Figure S6) as a function of (a) temperature at a H_2/NH_3 ratio of 1.0 and (b) H_2/NH_3 ratio at a temperature of 200 °C. The adsorbed species *OH, H_2O*, NH_2*, N_2*, and H* have negligible coverage at H_2/NH_3 = 1.0 with increasing temperature; N* and O* become negligible with the increasing H_2/NH_3 ratio. The evolution of free sites is shown on the twin axis in cyan color.
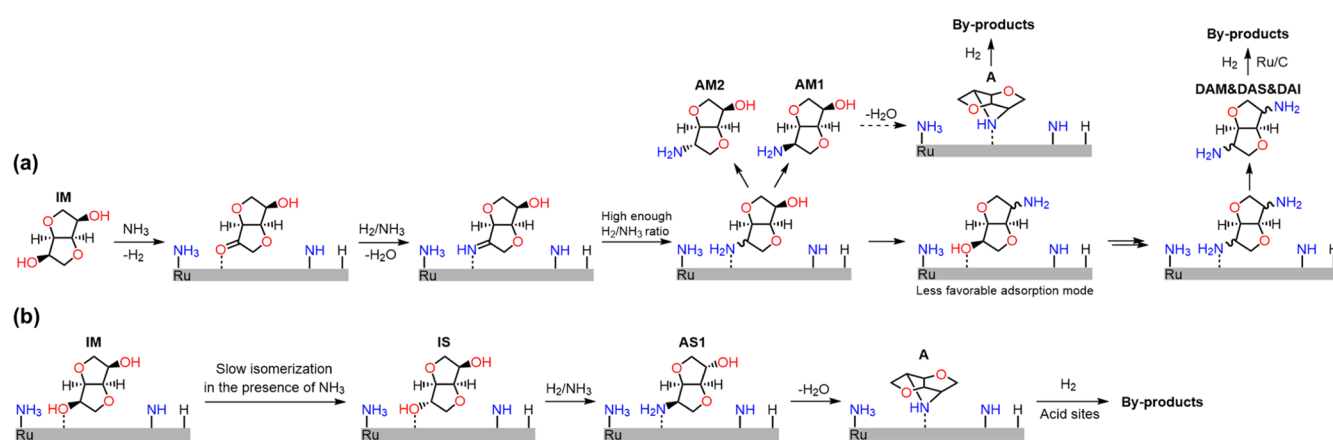
Figure 12. Proposed reaction pathways for the amination of IM with NH_3 over Ru/C in the presence of H_2. (a) Direct amination of IM and (b) IM isomerization to IS, followed by direct amination.

was evaluated at increasing temperatures for a H_2/NH_3 ratio of 1.0 and at increasing H_2/NH_3 ratios at 200 °C. As shown in Figure 11, poisoning by NH* and N* increases with temperature but can be reduced by increasing the H_2/NH_3 ratio. More details about the micro-kinetic analysis can be found in the Supporting Information.

Combining the above insights from modeling with the experimental investigations, we can rationalize how NH_3 and H_2 control the fate of isomannide IM over Ru/C during amination, as summarized in Figure 12a. Both the isomerization and amination of IM share the same first step, namely the dehydrogenation of one OH group into a chemisorbed ketone. We have already shown that isomerization is accelerated by exogenous H_2 due to co-adsorption of the substrate with H on the catalyst surface.[35] In the presence of both NH_3 and H_2, the main surface species are NH_3 and NH, instead of H, according to combined DFT calculations and micro-kinetics (Figure 11), which modifies the catalytic properties of Ru/C, thus strongly inhibiting the isomerization of IM to IS (Figure 8). This high coverage in NH species is also in agreement with adsorption experiments dosing NH_3 on Ru(0001).[40,41] A high NH and/or NH_3 coverage should also facilitate imine production on the catalyst, with its hydrogenation being limited by the H_2 coverage. As a matter of fact, a H_2 pressure of at least 5 bar is necessary to accelerate imine hydrogenation and reach 70% conversion of IM within 18 h (Figure 6). However, the H_2/NH_3 ratio needs to be kept low to prevent carbon loss. Indeed, as depicted in Figure 9, removing NH_3 and keeping H_2 is detrimental to the stability of aminoalcohols and diamines. Finally, to obtain diamines, aminoalcohols need to bind through their −OH group, which is less likely than through their −NH_2 group, discouraging their further amination.

In parallel, even though adsorbed amine species slow down the isomerization of the isohexides, IM is still slowly converted to IS. The latter then transforms into AS1, which is regarded as the precursor of tricyclic amine A, which is further converted into byproducts (Figure 12b).

◼ CONCLUSIONS

To conclude, the direct amination of isohexides with NH_3 favors the synthesis of aminoalcohols over Ru/C to the detriment of diamines. The key to this behavior is the inhibition of isomerization during amination (i.e., under NH_3), with *endo*-OH groups in isosorbide and isomannide showing much higher reactivity than *exo*-OH groups. In contrast, *exo*-

OH groups exhibit partial reactivity in isosorbide and isomannide isomerization under H_2 (i.e., without NH_3).

Isohexide diamines can be obtained in moderate yield by the direct amination of isomannide with NH_3 over Ru/C. A panel of byproducts is obtained, which could be generated by hydrolysis and hydrodeoxygenation from a tricyclic amine, as determined by MS. Increasing the NH_3 concentration (relative to that of H_2) poisons the Ru surface because of strong NH_3 adsorption and the concomitant generation of surface NH species. Furthermore, the isomerization of isomannide is hindered, thus avoiding the formation of AS1 and limiting, in turn, the carbon loss. Increasing the H_2 pressure accelerates the amination of isohexides, but too high a pressure is to be avoided to limit AM1 formation and, in turn, the promotion of hydrolysis and hydrodeoxygenation reactions of the intermediate compound A. Therefore, the ratio of H_2 to NH_3, which conditions the distribution of NH_2 and NH species on the Ru surface, drastically influences the catalytic performance.

All in all, we rationalize why the direct amination of isohexides to diamines over Ru/C is discouraged, as desirable as this reaction may be from an industrial point of view. The impossibility of obtaining high yields of diamines, even when starting from isomannide with two more reactive *endo*-OH groups, results from catalyst poisoning caused by ammonia and the formation of byproducts by hydrogenolysis. In the case of isosorbide and isoidide, the isomerization of the less reactive *exo*-OH groups to more reactive *endo*-OH groups is suppressed by ammonia and product amines.

■ EXPERIMENTAL SECTION

Chemicals. Isoidide (98%) was purchased from FluoroChem. Isosorbide (98%) and isomannide (95%) were procured from Sigma-Aldrich. Aqueous ammonia (25 wt %) was procured from Merck. AS1 and DAS were synthesized by ChemPartner. Unless otherwise stated, all chemicals were used without any further purification. An activated carbon-supported ruthenium (Ru/C, 5 wt %, reduced) catalyst was purchased from Sigma-Aldrich.

General Procedure for Amination Reactions. The high-pressure amination reactions were carried out in a Parr 5000 Multiple Reactor System (75 mL) equipped with a thermocouple and a digital manometer. In a typical reaction with aqueous NH_3, 1 g (6.8 mmol) of either IS, IM, or II, 0.2 g of Ru/C, and 15 mL of aqueous NH_3 (25 wt %, 0.91 g mL^{-1}, 0.2 mol of NH_3) were added to the reactor. The reactor was then sealed, flushed 3 times with H_2, and sealed at the target H_2 pressure and temperature. After the reaction, the reactor was cooled down to room temperature using an ice−water mixture, and the internal pressure was released.

General Procedure for the Synthesis of Isohexide *endo*-OH Monoketone. The oxidation of isohexides was performed in a 50 mL double-neck flask. Typically, 1 g substrate, 15 mL H_2O and 0.2 g Pt−Bi/C were added to the flask. An airflow [80 mL(STP)/min] was introduced to the suspension, and the reaction temperature was set to 60 °C. The *endo*-OH monoketone MK1 together with the diketone DK and was obtained after 72 h starting from IM at full conversion.

Identification of Products and Quantification. The crude product was filtered (perfluoroethylene, 0.2 μm) to remove the catalyst and was diluted in methanol. The mixture was analyzed by gas chromatography using a Bruker Scion 436 GC equipped with an Agilent HP-5MS column (30 m × 0.25 mm x 0.25 μm), a flame ionization detector (FID), and an autosampler. The calibration was performed using *n*-dodecanol as the internal standard.

GC methods A and B (see Figure S8 in the Supporting Information) were used to identify all possible products in the isomerization and amination of isohexides (Schemes 1 and 2). Representative GC spectra of the product mixture obtained from the amination of IS or IM are provided in Figure S9. The quantification of

Scheme 2. Possible Products Obtained from the Dehydrogenation of Isohexides and Reductive Amination of Isohexide Monoketones
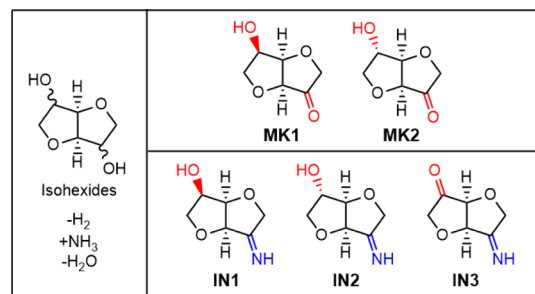
each substrate and conversion was carried out using method A, while method B was used to measure the molar ratio between DAI and AS1. Equal GC response factors was assumed for isohexides and the corresponding alcoholamines and diamines.

GC methods A and C (see Figure S10 in the Supporting Information) were used to identify the products in the oxidation of IM and IS, respectively. Representative GC spectra of the product mixture after oxidation are provided in Figure S11. Equal GC response factors were assumed for isohexides and ketones.

In each experiment, the substrate conversion and yield of each product were calculated using the following expressions

$$\text{Conversion} = \left(1 - \frac{n_a}{n_0}\right) \times 100\% \tag{1}$$

$$\text{Yield} = \frac{n_p}{n_0} \times 100\% \tag{2}$$

where n_a is the molar amount of reactant after reaction, n_0 is the initial molar amount of reactant, and n_p is the molar amount of product after reaction.

MS analysis was used to measure the molecular weight of the possible byproducts during the amination reaction. The analyses were conducted using a Thermo QExactive mass spectrometer (Source-type ESI, scan began at m/z 50, scan ended at m/z 1000, and ion polarity, positive or negative).

Computational Details. DFT implemented in Gaussian 16[42] was used to investigate the thermodynamic stability of isohexides and their potential amination products using the MO6-2X functional[43] with the def2-TZVPP basis set.[44,45] SCF convergence and optimization criteria were set to tight, and the obtained optimized geometries were used to calculate the vibrational frequencies. These were subsequently used to calculate standard Gibbs free energies at 200 °C and 101 kPa using the GoodVibes python package under the harmonic ideal gas approximation.[44−46] After an initial rescaling of the normal modes recommended for the selected level of theory,[47] frequencies below 100 cm^{-1} were rescaled to 100 cm^{-1} for a quasi-harmonic treatment of both vibrational entropy[48] and vibrational enthalpy.[49]

For the study of on−surface reactions, periodic DFT, as implemented in the Vienna ab initio simulation package (VASP)[50] was used to investigate reaction pathways for various reaction species. Electronic energies were approximated at the GGA level using the Perdew−Burke−Ernzerhof (PBE)[51] exchange−correlation functional with dDSc dispersion correction.[52] Ion-electron interactions were treated using the Projector Augmented Wave (PAW) formalism[53,54] with an 850 eV cutoff for the augmentation charges, and the plane-wave basis set was truncated at 500 eV. The Ru catalyst was modeled by a 4 layer thick $p(4 \times 4)$ slab of Ru(0001) surface. The slab was cleaved from bulk Ru following a full optimization of the bulk, which resulted in lattice parameters of a = 2.702 Å and c/a ratio of 1.578. The bottom two layers were kept frozen in their bulk positions, while all other degrees of freedom were allowed to relax until the forces were lower than 0.01 eV Å^{-1} The cutoff for the electronic self-consistency cycle was set to 10^{-7} eV. The calculations for slab or slab-
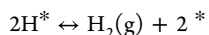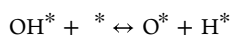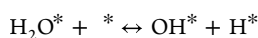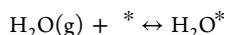
adsorbate systems used a Gamma-centered $5 \times 5 \times 1$ k-point mesh to sample the Brillouin zone. Second order Methfessel-Paxton smearing scheme, AM2, was employed with a smearing width of 0.2 eV. To minimize the interactions between the different periodic images of the system in the direction normal to the slab, a minimum vacuum gap of 25 Å augmented by a dipole correction of both energy and forces was implemented in the given direction. The O−H transition states for IM and aminoalcohols were computed using a combination of DIMER and quasi-Newton methods.
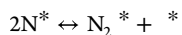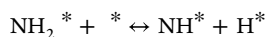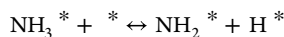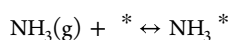
Thermal and entropic contributions to the total energy were estimated under the harmonic approximation by calculating the normal modes for the adsorbate part of all reaction species using central finite differences with a step size of 0.01 Å. All normal modes (those with a vibration below 100 cm^{-1} were rescaled to 100 cm^{-1} to avoid spurious effects within the harmonic approximation) were used to calculate the zero-point energy (ZPE) and other thermal and entropic contributions under harmonic and ideal gas approximations.

The molecular species were optimized at the Gamma point in a $20 \times 20 \times 20$ Å^3 cubic box. Due to the polarity of the molecules, dipole correction was used in all directions. A reduced smearing width of 0.02 eV was employed for molecular species. The vibrational, rotational, and translational contributions to the enthalpy and entropy were calculated under the harmonic ideal gas approximation, taking into account the proper symmetry of the molecules.

The kinetic analysis was performed for two cases: surface coverage vs temperature and surface coverage vs NH$_3$/H$_2$ molar ratio. In the former case, the kinetic equations were solved to find the steady state for an initial condition of 25 wt % aqueous NH$_3$ in a 15 mL reactor and a H$_2$/NH$_3$ ratio of 1.0; this sets the initial molar concentrations of NH$_3$, H$_2$O, and H$_2$ gas phase species. In the latter case, the same initial condition for NH$_3$ was used, and the H$_2$ concentration was set according to the H$_2$/NH$_3$ ratio. The initial concentration of N$_2$ gas was set to 0.0 molar in both cases. The binding energy of H* was scaled by 0.12 eV ($\sim$20%) to take into account the lateral interactions in a mean-field approximation. The binding energy of H* was rescaled by $\sim$20% to mimic the lateral interactions in a mean-field approximation. However, little to no effect was found on the steady-state kinetics as a result of this rescaling. Figure S12 shows the steady-state coverage of surface species and empty sites as a function of temperature at a H$_2$/NH$_3$ ratio of 1.0 when H* is not rescaled, while Figure S13 shows the evolution of N$_2$ gas as a function of temperature for a H$_2$/NH$_3$ ratio of 1.0.

The following elementary reactions were considered

$$NH_3(g) + {}^* \leftrightarrow NH_3{}^*$$

$$NH_3{}^* + {}^* \leftrightarrow NH_2{}^* + H^*$$

$$NH_2{}^* + {}^* \leftrightarrow NH^* + H^*$$

$$NH^* + {}^* + {}^* \leftrightarrow N^* + H^*$$

$$2N^* \leftrightarrow N_2{}^* + {}^*$$

$$N_2{}^* \leftrightarrow N_2(g) + {}^*$$

$$H_2O(g) + {}^* \leftrightarrow H_2O^*$$

$$H_2O^* + {}^* \leftrightarrow OH^* + H^*$$

$$OH^* + {}^* \leftrightarrow O^* + H^*$$

$$2H^* \leftrightarrow H_2(g) + 2{}^*$$
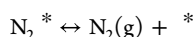
The differential equations resulting from the elementary steps were solved using the find_steady_state subroutine implemented in the Micki program[55] with dt = 200 and a tolerance of 1×10^{-8}. Adsorption of gas-phase species was modeled using a non-interacting 2D ideal gas (defined as the STICK method in Micki) and on−surface reactions were modeled using the Transition State Theory (defined as the TST method in Micki). A continuous stirred reactor (CSTR) with an infinite flowrate (i.e., a perfect mixture) was achieved by fixing the concentrations of NH$_3$(g), H$_2$O(g), and H$_2$(g).

■ ASSOCIATED CONTENT

ⓈI Supporting Information

The Supporting Information is available free of charge at https://pubs.acs.org/doi/10.1021/acssuschemeng.2c07501.

Coordinates for DFT calculations (ZIP)
Blank mass spectra of the MS system; mass spectra of AS2 and DAS; mass spectra of the reaction mixture after amination of isomannide IM under 30 bar H$_2$; possible byproducts from IM amination; reductive amination of *endo*-OH ketone mixtures; optimized structures for different adsorption modes of aminoalcohols through either −OH or −NH$_2$ functional groups; reaction profile corresponding to the dehydrogenation of NH$_3$ to form NH$_x$ species on Ru(0001); GC methods A and B used for the analysis of product mixtures in the amination of IM; representative GC chromatograms obtained for reactant and product analysis using GC methods A and B; GC method C used for the analysis of product mixtures in the oxidation of IM and IS; representative GC chromatograms obtained for reactant and product analysis using GC methods A and C; steady-state coverage of surface species and empty catalytic sites as a function of temperature at a H$_2$/NH$_3$ ratio of 1.0; evolution of N$_2$ gas as a function of temperature for H$_2$/NH$_3$ molar ratio of 1.0; and a table listing substrate conversion and product yield for figures in the main text (PDF)

■ AUTHOR INFORMATION

Corresponding Authors

Raphael Wischert − *Eco-Efficient Products and Processes Laboratory (E2P2L), UMI 3464 CNRS-Solvay, 201108 Shanghai, China*; Email: raphael.wischert@solvay.com

Carine Michel − *Université de Lyon, Ecole Normale Supérieure de Lyon, CNRS UMR 5182, Laboratoire de Chimie, F69364 Lyon, France*; ⓞ orcid.org/0000-0002-4501-7194; Email: carine.michel@ens-lyon.fr

Karine de Oliveira Vigier − *IC2MP UMR CNRS_Université de Poitiers 7285, ENSIP 1 rue Marcel Doré, 86073 Poitiers Cedex 9, France*; ⓞ orcid.org/0000-0003-3613-7992; Email: karine.vigier@univ-poitiers.fr

Marc Pera-Titus − *Eco-Efficient Products and Processes Laboratory (E2P2L), UMI 3464 CNRS-Solvay, 201108 Shanghai, China; Cardiff Catalysis Institute, School of Chemistry, Cardiff University, CF10 3AT Cardiff, U.K.*; ⓞ orcid.org/0000-0001-7335-1424; Email: peratitusm@cardiff.ac.uk

Authors

Hang Hu − *Eco-Efficient Products and Processes Laboratory (E2P2L), UMI 3464 CNRS-Solvay, 201108 Shanghai, China; IC2MP UMR CNRS_Université de Poitiers 7285, ENSIP 1 rue Marcel Doré, 86073 Poitiers Cedex 9, France*

Muhammad Akif Ramzan − *Université de Lyon, Ecole Normale Supérieure de Lyon, CNRS UMR 5182, Laboratoire de Chimie, F69364 Lyon, France*; ⓞ orcid.org/0000-0002-1369-6356

François Jerôme − *IC2MP UMR CNRS_Université de Poitiers 7285, ENSIP 1 rue Marcel Doré, 86073 Poitiers Cedex 9, France*; ⓞ orcid.org/0000-0002-8324-0119

Complete contact information is available at:
https://pubs.acs.org/10.1021/acssuschemeng.2c07501

Author Contributions

[⊥]H.H. and M.A.R. contributed equally to this work. The manuscript was written through contributions of all authors. All authors have given approval to the final version of the manuscript.

Notes

The authors declare no competing financial interest.

■ ABBREVIATIONS

DAM, diaminoisomannide; DAS, diaminoisosorbide; DAI, diaminoisoidide; AM1, aminoisomannide; AM2, *exo*-NH$_2$-aminoisosorbide; AS1, *exo*-OH-aminoisosorbide; AS1, *exo*-OH-aminoisosorbide; AS2, aminoiidide; II, isoidide; IM, isomannide; IS, isosorbide

■ REFERENCES

(1) Wittcoff, H. A.; Reuben, B. G.; Plotkin, J. S. *Industrial Organic Chemicals*. 2nd ed., Wiley, NY, 2004.

(2) Lawrence, S. A. *Amines: Synthesis, Properties and Applications*; Cambridge University Press, 2004.

(3) Roose, P.; Eller, K.; Henkes, E.; Rossbacher, R.; Höke, H. *Amines, Aliphatic, Ullmann's Encyclopedia of Industrial Chemistry*; Wiley-VCH: Weinheim, 2015, p 1.

(4) Imm, S.; Bahn, S.; Zhang, M.; Neubert, L.; Neumann, H.; Klasovsky, F.; Pfeffer, J.; Haas, T.; Beller, M. Improved ruthenium-catalyzed amination of alcohols with ammonia: synthesis of diamines and amino esters. *Angew. Chem., Int. Ed.* 2011, 50, 7599−7603.

(5) Delidovich, I.; Hausoul, C.; Deng, L.; Pfützenreuter, R.; Rose, M.; Palkovits, R. Alternative Monomers Based on Lignocellulose and Their Use for Polymer Production. *Chem. Rev.* 2016, 116, 1540−1599.

(6) Pelckmans, M.; Renders, T.; Van de Vyver, S.; Sels, B. F. Bio-based amines through sustainable heterogeneous catalysis. *Green Chem.* 2017, 19, 5303−5331.

(7) Pelckmans, M.; Vermandel, W.; Van Waes, F.; Moonen, K.; Sels, B. F. Low-temperature reductive aminolysis of carbohydrates to diamines and aminoalcohols by heterogeneous catalysis. *Angew. Chem. Int. Ed* 2017, 56, 14540−14544.

(8) Froidevaux, V.; Negrell, C.; Caillol, S.; Pascault, J.-P.; Boutevin, B. Biobased Amines: From Synthesis to Polymers; Present and Future. *Chem. Rev.* 2016, 116, 14181−14224.

(9) Brun, N.; Hesemann, P.; Esposito, D. Expanding the biomass derived chemical space. *Chem. Sci.* 2017, 8, 4724−4738.

(10) Liang, G.; Wang, A.; Li, L.; Xu, G.; Yan, N.; Zhang, T. Production of primary amines by reductive amination of biomass-derived aldehydes/ketones. *Angew. Chem., Int. Ed.* 2017, 56, 3050−3054.

(11) Flèche, G.; Huchette, M. Preparation, properties and chemistry. *Starch/Stärke* 1986, 38, 26−30.

(12) Wiggins, L. F. 2. The anhydrides of polyhydric alcohols. Part I. The constitution of isomannide. *J. Chem. Soc.* 1945, 4−7.

(13) Rose, M.; Palkovits, R. Isosorbide as a renewable platform chemical for versatile applications − *quo vadis*? *ChemSusChem* 2012, 5, 167−176.

(14) Fenouillot, F.; Rousseau, A.; Colomines, G.; Saint-Loup, R.; Pascault, J. P. Polymers from renewable 1,4:3,6-dianhydrohexitols (isosorbide, isomannide and isoidide): a review. *Progr. Polym. Sci.* 2010, 35, 578−622.

(15) Wu, J.; Jasinska-Walc, L.; Dudenko, D.; Rozanski, A.; Hansen, M. R.; van Es, D.; Koning, C. E. An investigation of polyamides based on isoidide-2,5-dimethyleneamine as a green rigid building block with enhanced reactivity. *Macromolecules* 2012, 45, 9333−9346.

(16) Montgomery, R.; Wiggins, L. F. 77. The anhydrides of polyhydric alcohols. Part IV. The constitution of dianhydro sorbitol. *J. Chem. Soc.* 1946, 390−393.

(17) Fletcher, H. G., Jr; Goepp, R. M., Jr Hexitol Anhydrides.[1] 1,4,3,6-Dianhydro-L-iditol and the Structures of Isomannide and Isosorbide. *J. Am. Chem. Soc.* 1946, 68, 939−941.

(18) Fletcher, H. G., Jr; Goepp, R. M., Jr 1,4;3,6-Hexitol dianhydride L-isoidide. *J. Am. Chem. Soc.* 1945, 67, 1042−1043.

(19) Cope, C.; Shen, T. Y. The stereochemistry of 1,4: 3,6-dianhydrohexitol derivatives. *J. Am. Chem. Soc.* 1956, 78, 3177−3182.

(20) Brimacombe, J.; Foster, A. B.; Stacey, M.; Whiffen, D. H. Aspects of stereochemistry − I: Properties and reactions of some diols. *Tetrahedron* 1958, 4, 351−360.

(21) Montgomery, R.; Wiggins, L. F. 78. The anhydrides of polyhydric alcohols. Part V. 2 : 5-Diamino 1 : 4−3 : 6-dianhydro mannitol and sorbitol and their sulphanilamide derivatives. *J. Chem. Soc.* 1946, 0, 393−396.

(22) Bashford, V. G.; Wiggins, L. F. 82. Anhydrides of polyhydric alcohols. Part XIII. The amino-derivatives of 1 : 4−3 : 6-dianhydro-mannitol, -sorbitol, and -L-iditol, and their behaviour towards nitrous acid. *J. Chem. Soc.* 1950, 0, 371−374.

(23) Thiyagarajan, S.; Gootjes, L.; Vogelzang, W.; Wu, J.; van Haveren, J.; van Es, D. S. Chiral building blocks from biomass: 2,5-diamino-2,5-dideoxy-1,4-3,6-dianhydroiditol. *Tetrahedron* 2011, 67, 383−389.

(24) Thiyagarajan, S.; Gootjes, L.; Vogelzang, W.; van Haveren, J.; Lutz, M.; van Es, D. S. Renewable rigid diamines: efficient, stereospecific synthesis of high purity isohexide diamines. *ChemSusChem* 2011, 4, 1823−1829.

(25) Kuszmann, J.; Medgyes, G. Synthesis and biological activity of 1,4:3,6-dianhydro-2,5-diazido-2,5-dideoxyhexitols. *Carbohydr. Res.* 1980, 85, 259−269.

(26) Bähn, S.; Imm, S.; Neubert, L.; Zhang, M.; Neumann, H.; Beller, M. The catalytic amination of alcohols. *ChemCatChem* 2011, 3, 1853−1864.

(27) Pera-Titus, M.; Shi, F. Catalytic amination of biomass-based alcohols. *ChemSusChem* 2014, 7, 720−722.

(28) Pingen, D.; Diebolt, O.; Vogt, D. Direct amination of bio-alcohols using ammonia. *ChemCatChem* 2013, 5, 2905−2912.

(29) Wright, L. W.; Brandner, J. D. Catalytic Isomerization of Polyhydric Alcohols.[1] II. The Isomerization of Isosorbide to Isomannide and Isoidide. *J. Org. Chem.* 1964, 29, 2979−2982.

(30) Brandner, D.; Wright, L. W. Process for producing isoidide. U.S. Patent no. 3,023,223 A, 1962.

(31) Schelwies, M.; Brinks, M.; Schaub, T.; Melder, J.-P.; Paciello, R.; Merger, M. Process for the homogeneously catalyzed amination of alcohols with ammonia in the presence of a complex catalyst which comprises nonanionic ligands. Patent no. WO 2014016241 A1 2014

(32) Bahé, F.; Grand, L.; Cartier, E.; Jacolot, M.; Moebs-Sanchez, S.; Portinha, D.; Fleury, E.; Popowycz, F. Direct amination of isohexides via borrowing hydrogen methodology: regio- and stereoselective issues. *Eur. J. Org. Chem.* 2020, 2020, 599−608.

(33) Pfützenreuter, R.; Rose, M. Aqueous-phase amination of biogenic isohexides by using Ru/C as a solid catalyst. *ChemCatChem* 2016, 8, 251−255.

(34) Niemeier, J.; Engel, R. V.; Rose, M. Is water a suitable solvent for the catalytic amination of alcohols? *Green Chem.* **2017**, *19*, 2839−2845.

(35) Hu, H.; Ramzan, A.; Wischert, R.; Jerôme, F.; Michel, C.; de Olivera Vigier, K.; Pera-Titus, M. Pivotal role of H_2 in the isomerisation of isosorbide over a Ru/C catalyst. *Catal. Sci. Technol.* **2021**, *11*, 7973−7981.

(36) Hausoul, P. J. C.; Negahdar, L.; Schute, K.; Palkovits, R. Unravelling the Ru-catalyzed hydrogenolysis of biomass-based polyols under neutral and acidic conditions. *ChemSusChem* **2015**, *8*, 3323−3330.

(37) Wang, T.; Ibañez, J.; Wang, K.; Fang, L.; Sabbe, M.; Michel, C.; Paul, S.; Pera-Titus, M.; Sautet, P. Rational design of selective metal catalysts for alcohol amination with ammonia. *Nat. Catal.* **2019**, *2*, 773−779.

(38) Honkala, K.; Hellman, A.; Remediakis, I. N.; Logadottir, A.; Carlsson, A.; Dahl, S.; Christensen, C. H.; Nørskov, J. K. Ammonia synthesis from first-principles calculations. *Science* **2005**, *307*, 555−558.

(39) Lu, X.; Zhang, J.; Chen, W.-K.; Roldan, A. Kinetic and mechanistic analysis of NH_3 decomposition on Ru(0001), Ru(111) and Ir(111) surfaces. *Nanoscale Adv* **2021**, *3*, 1624−1632.

(40) Benndorf, C.; Madey, T. E. Adsorption and orientation of NH3 on Ru(001). *Surf. Sci.* **1983**, *135*, 164−183.

(41) Carabineiro, S. A. C.; Matveev, A. V.; Gorodetskii, V. V.; Nieuwenhuys, B. E. Selective oxidation of ammonia over Ru(0001). *Surf. Sci.* **2004**, *555*, 83−93.

(42) Frisch, M. J.; Trucks, G. W.; Schlegel, H. B.; Scuseria, G. E.; Robb, M. A.; Cheeseman, J. R.; Scalmani, G.; Barone, V.; Mennucci, B.; Petersson, G. A.; Nakatsuji, H.; Caricato, M.; Li, X.; Hratchian, H. P.; Izmaylov, A. F.; Bloino, J.; Zheng, G.; Sonnenberg, J. L.; Hada, M.; Ehara, M.; Toyota, K.; Fukuda, R.; Hasegawa, J.; Ishida, M.; Nakajima, T.; Honda, Y.; Kitao, O.; Nakai, H.; Vreven, T.; Montgomery, J. A., Jr; Peralta, J. E.; Ogliaro, F.; Bearpark, M.; Heyd, J. J.; Brothers, E.; Kudin, K. N.; Staroverov, V. N.; Kobayashi, R.; Normand, J.; Raghavachari, K.; Rendell, A.; Burant, J. C.; Iyengar, S. S.; Tomasi, J.; Cossi, M.; Rega, N.; Millam, J. M.; Klene, M.; Knox, J. E.; Cross, J. B.; Bakken, V.; Adamo, C.; Jaramillo, J.; Gomperts, R.; Stratmann, R. E.; Yazyev, O.; Austin, A. J.; Cammi, R.; Pomelli, C.; Ochterski, J. W.; Martin, R. L.; Morokuma, K.; Zakrzewski, V. G.; Voth, G. A.; Salvador, P.; Dannenberg, J. J.; Dapprich, S.; Daniels, A. D.; Farkas, O.·.; Foresman, J. B.; Ortiz, J. V.; Cioslowski, J.; Fox, D. J. *Gaussian 09*; Gaussian, Inc.: Wallingford, CT, 2016.

(43) Zhao, Y.; Truhlar, D. G. The M06 suite of density functionals for main group thermochemistry, thermochemical kinetics, non-covalent interactions, excited states, and transition elements: Two new functionals and systematic testing of four M06-class functionals and 12 other functionals. *Theor. Chem. Acc.* **2008**, *120*, 215−241.

(44) Weigend, F.; Ahlrichs, R. Balanced basis sets of split valence, triple zeta valence and quadruple zeta valence quality for H to Rn: Design and assessment of accuracy. *Phys. Chem. Chem. Phys.* **2005**, *7*, 3297−3305.

(45) Weigend, F.; Ahlrichs, R. Accurate Coulomb-fitting basis sets for H to Rn. *Phys. Chem. Chem. Phys.* **2006**, *8*, 1057−1065.

(46) Luchini, G.; Alegre-Requena, J. V.; Funes-Ardoiz, I.; Paton, R. S. *GoodVibes: automated thermochemistry for heterogeneous computational chemistry data*; F1000 Research Ltd, 2020, Vol 9.

(47) Alecu, I. M.; Zheng, J.; Zhao, Y.; Truhlar, D. G. Computational thermochemistry: scale factor databases and scale factors for vibrational frequencies obtained from electronic model chemistries. *J. Chem. Theory Comput.* **2010**, *6*, 2872−2887.

(48) Ribeiro, R. F.; Marenich, A. V.; Cramer, C. J.; Truhlar, D. G. Use of solution-phase vibrational frequencies in continuum models for the free energy of solvation. *J. Phys. Chem. B* **2011**, *115*, 14556−14562.

(49) Li, Y.-P.; Gomes, J.; Mallikarjun Sharada, S.; Bell, A. T.; Head-Gordon, M. Improved force-field parameters for QM/MM simulations of the energies of adsorption for molecules in zeolites and a free rotor correction to the rigid rotor harmonic oscillator model for adsorption enthalpies. *J. Phys. Chem. C* **2015**, *119*, 1840−1850.

(50) Kresse, G.; Furthmüller, J. Efficient iterative schemes for ab initio total-energy calculations using a plane-wave basis set. *J. Phys. Rev. B* **1996**, *54*, 11169−11186.

(51) Perdew, J. P.; Burke, K.; Ernzerhof, M. Generalized gradient approximation made simple. *Phys. Rev. Lett.* **1996**, *77*, 3865−3868.

(52) Steinmann, S.; Corminboeuf, C. A generalized-gradient approximation exchange hole model for dispersion coefficients. *J. Chem. Phys.* **2011**, *134*, 044117.

(53) Blöchl, P. E. Projector augmented-wave method. *Phys. Rev. B* **1994**, *50*, 17953−17979.

(54) Kresse, G.; Joubert, D. From ultrasoft pseudopotentials to the projector augmented-wave method. *Phys. Rev. B* **1999**, *59*, 1758−1775.

(55) Hermes, E. D.; Janes, A. N.; Schmidt, J. R. M. Micki: A python-based object-oriented microkinetic modeling code. *J. Chem. Phys.* **2019**, *151*, 014112.